Release of N_2 from the Carbon Nanotubes via High-Temperature Annealing

Hyun Chul Choi, Seung Yong Bae, Woo-Sung Jang, and Jeunghee Park*

Department of Chemistry, Korea University, Jochiwon 339-700, South Korea

Ha Jin Song and Hyun-Joon Shin

Pohang Accelerator Laboratory and Department of Physics, Pohang University of Science and Technology, San 31, Hyojadong, Pohang 790-784, South Korea

Hyunsung Jung and Jae-Pyoung Ahn

Nano-Material Research Center, Korea Institute of Science and Technology, Seoul 136-791, South Korea

Received: August 29, 2004; In Final Form: November 4, 2004

Nitrogen (N)-doped carbon nanotubes (CNTs) were heated to 1000 °C under an ultrahigh vacuum. X-ray photoelectron spectroscopy (XPS) and X-ray absorption near-edge structure (XANES) reveal three different N structures; graphitelike, pyridine-like, and molecular N_2. The vibrationally resolved XANES peaks of N_2 were first observed, suggesting the existence of molecular N_2 as intercalated and trapped forms. The annealing process can decrease the average N content from 6.3 at. % to 3.3 at. %, mainly by releasing molecular N_2. Electron energy-loss spectroscopy (EELS) confirms that the annealing releases molecular N_2 from the CNTs.

I. Introduction

Carbon nanotubes (CNTs) are currently the subject of intense research, because of their unique structural, electrical, and mechanical properties.[1] They can be remarkably either metallic or semiconducting, depending on their helicity and diameter.[2] Because the CNTs are now widely accepted as a promising material for nano-electronic devices[3,4] and electron field emission sources,[5] the control of electrical properties has become a very important subject. The doping of CNTs with N atoms is one of practical and feasible ways to tailor their electrical properties to a metallic material. Much attention has been directed to reveal the electronic structures of the N-doped CNTs. The diverse structures such as graphitelike (N atoms replacing C atoms in graphite layers), pyridine-like, pyrrolic, cross-linked sp^3 structures, and gaseous N_2 were identified by electron energy-loss spectroscopy (EELS) and X-ray photolelectron spectroscopy (XPS).[6−11] Despite those tremendous works, however, there is no definite answer for whether all those N structures are allowed in the CNTs.

The main object of the present study is to understand the electronic structures of doped N atoms in the CNTs better. We prepared vertically aligned multiwalled N-doped CNTs via a pyrolysis of iron phthalocyanine ($FeC_{32}N_8H_{16}$, designated as FePc hereafter) at 900 °C. The CNTs then were heated at various temperatures, up to 1000 °C. We focus the high-temperature annealing effect on the electronic structures of N atoms, providing more-precise structure assignments with their thermal stability. In fact, the heating is a popular purification method for CNTs that are contaminated with many impurities such as metal catalysts or amorphous carbons.[12,13] However, there still are few works on how much the heating process can modify the electronic structures of CNTs. X-ray photoelectron spectroscopy (XPS), X-ray absorption near-edge structure (XANES), and electron energy-loss spectroscopy (EELS) were used to study the electronic structures of the N atoms. The XPS technique is one of the best methods for obtaining information about the occupied electronic structures and chemical bonding states of atoms. On the other hand, XANES provides important information about the unoccupied electronic structure of the X-ray absorbing elements.[14] When a system has π-bonds, one can find a sharp 1s $\rightarrow \pi^*$ transition, providing unambiguous information on the local structure around an atom of interest. The EELS provides the electronic states of N atoms in an individual nanotube, although the resolution is lower than observed with XPS and XANES. By combining the XPS, XANES, and EELS results, we can discuss the variation of the electronic structures of as-grown and annealed CNTs and provide definite evidence for the release of molecular N_2 from the CNTs during the annealing process.

II. Experiment

The vertically aligned N-doped CNTs were grown on silicon oxide substrates by pyrolyzing FePc under an argon/hydrogen (Ar/H_2) flow at 900 °C.[15] The CNTs were heated resistively at various temperatures, up to 1000 °C, under a vacuum of $<10^{-8}$ Torr. The heating time at each temperature was 10 min. The temperature was estimated by a current−temperature calibration curve, with an uncertainty of ±30 °C. The size and morphology of as-grown and annealed CNTs were examined by scanning electron microscopy (SEM) (Hitachi model S-4300) and transmission electron microscopy (TEM) (JEOL model JEM-4010). The Raman spectrum was measured (Renishaw model RM1000) using the 514.5-nm line from an Ar^+ ion laser. EELS (Gatan model GIF-2000), coupled with TEM (FEI TECNAI G^2), was used.

The XPS measurement was performed at the 8A1 (undulator U7) beam line of the Pohang Light Source (PLS). The

* Author to whom correspondence should be addressed. E-mail address: parkjh@korea.ac.kr.

10.1021/jp046098b CCC: $30.25
Published on Web 01/12/2005

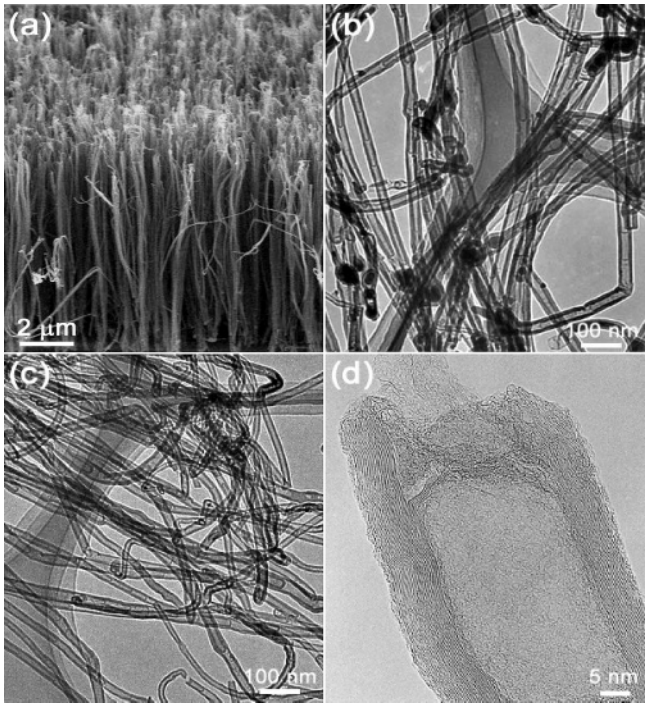

Figure 1. (a) Scanning electron microscopy (SEM) micrograph of vertically aligned N-doped CNTs. (b) Transmission electron microscopy (TEM) image showing the bamboolike structure of as-grown N-doped CNTs; the metal nanoparticles are frequently encapsulated in the CNTs. (c) TEM image for the annealed CNTs at 1000 °C, revealing no encapsulated metal nanoparticles. (d) High-resolution transmission eletron microscopy (HRTEM) image for open-edge parts of the annealed CNT at 1000 °C.

experiment was performed in an ultrahigh vacuum (UHV) chamber with a base pressure of $\leq 5 \times 10^{-10}$ Torr. The photoelectrons emitted from the surface of CNTs were collected and their energies were analyzed with an electron energy analyzer (Physical Electronics, Model PHI 3057 with a 16-channel detector). The photon energy was 1265 eV, in which the inelastic mean free path of photoelectrons from C 1s and N 1s is estimated to be ~2.7 and ~2.5 nm, respectively, using the formula given by Seah and Dench.[16] The binding energies were corrected for specimen charging by referencing the C 1s peak to 284.6 eV. The background was subtracted by Shirley's method,[17] and the spectrum deconvolution was performed by fitting the Voigt profiles. The XANES measurement was performed at the 8A1 beam line of PLS. The spectral resolving power ($E/\Delta E$) of incident photons is ~5000 at 400 eV. All spectra were taken with a total electron yield mode recording the sample current at room temperature. The photon energy was calibrated by the second peak in the π^* resonance of N_2 gas to be 401.1 eV as a reference. To eliminate the effect of incident beam intensity fluctuations and monochromator absorption features, all spectra were normalized by a reference signal from a gold mesh with 90% transmission.

III. Results and Discussion

Figure 1a shows the SEM image of the vertically aligned CNTs grown on a large area of the substrate. The average length of the CNTs is ~10 μm. The TEM image depicts the general morphology of as-grown CNTs (Figure 1b). The nanotubes exhibit exclusively a bamboolike structure in which the tube inside is separated into a series of compartments. The average diameter of CNTs is 50 nm, and the average wall thickness is 10 nm. The Fe nanoparticles are frequently encapsulated in the CNTs. Figure 1c shows the annealed CNTs at 1000 °C. The nanotubes still retain a bamboolike structure, with the same diameter and wall thickness. Few metal nanoparticles remain inside the CNTs. Figure 1d corresponds to the high-resolution TEM image for open-end parts of the annealed CNT. The highly crystalline graphitic sheets at the wall are aligned parallel to the tube axis. The tube opening probably results from the sublimation of encapsulated catalytic particles. Huang et al. reported that the heat treatment at a pressure of <10 Pa and a temperature of >1500 °C converts the trapped Fe−Mo catalytic nanoparticles into vapor and they escape from the CNTs.[13] We observed here that the catalytic nanoparticles inside the CNTs can be removed at the lower temperature. This may be due to the pressure being lower ($<1.1 \times 10^{-5}$ Pa) than that of Huang's experiment. We also believe that the increased vapor pressure of the Fe nanoparticles fractures the end of CNTs and then releases through the open end.

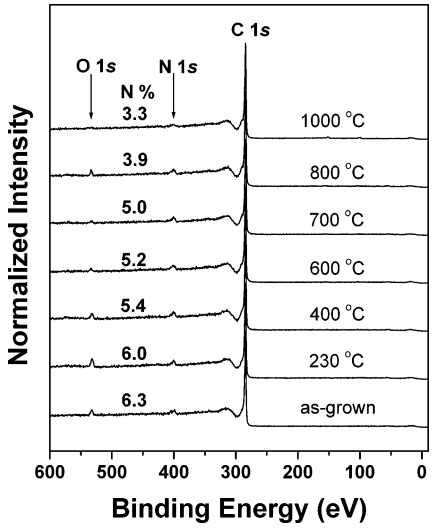

Figure 2. Full-range X-ray photoelectron spectroscopy (XPS) spectrum of the N-doped CNTs annealed at various temperatures up to 1000 °C. The N content decreases from 6.3 at. % to 3.3 at. % after heating at 1000 °C.

Figure 2 displays full-range XPS spectrum of the annealed CNTs at various temperatures. The XPS data shows distinct C, N, and O 1s peaks. No other elements were detected from the N-doped CNTs. The O peak would be originated from the oxygen contaminants and/or silicon oxide substrates. The N content, which is defined as the N/(C + N) atomic ratio (given as a percentage), was estimated by the area ratio of the N and C 1s peaks, taking into account their relative sensitivities. For the as-grown CNTs, the average N content is estimated as 6.3 at. %. As the annealing temperature increases to 1000 °C, the N content decreases gradually to 3.3 at. %. The O content is also reduced after each annealing step.

To investigate the electronic structures of C and N atoms, we obtained the fine-scanned C 1s and N 1s peaks. The C 1s spectrum of as-grown and annealed CNTs is displayed in Figure 3a, showing an asymmetric peak centered at 284.6 eV. As shown in Figure 3b, the C 1s peak can be deconvoluted into three bands: PC1, PC2, and PC3, at 284.5, 285.5, and 287 eV, respectively, corresponding to the C−C bonds in graphite, C−N bonds, and C−O bonds.[18,19] The area composition of PC1, PC2, and PC3 is 78%, 16%, and 6% for the as-grown CNTs and 82%, 13%, and 5% for the CNTs annealed at 1000 °C, respectively. With the annealing, the fraction of the PC1 graphite structures increases whereas that of the N-bonded structures (PC2) and O-bonded structure (PC3) decreases, indicating that

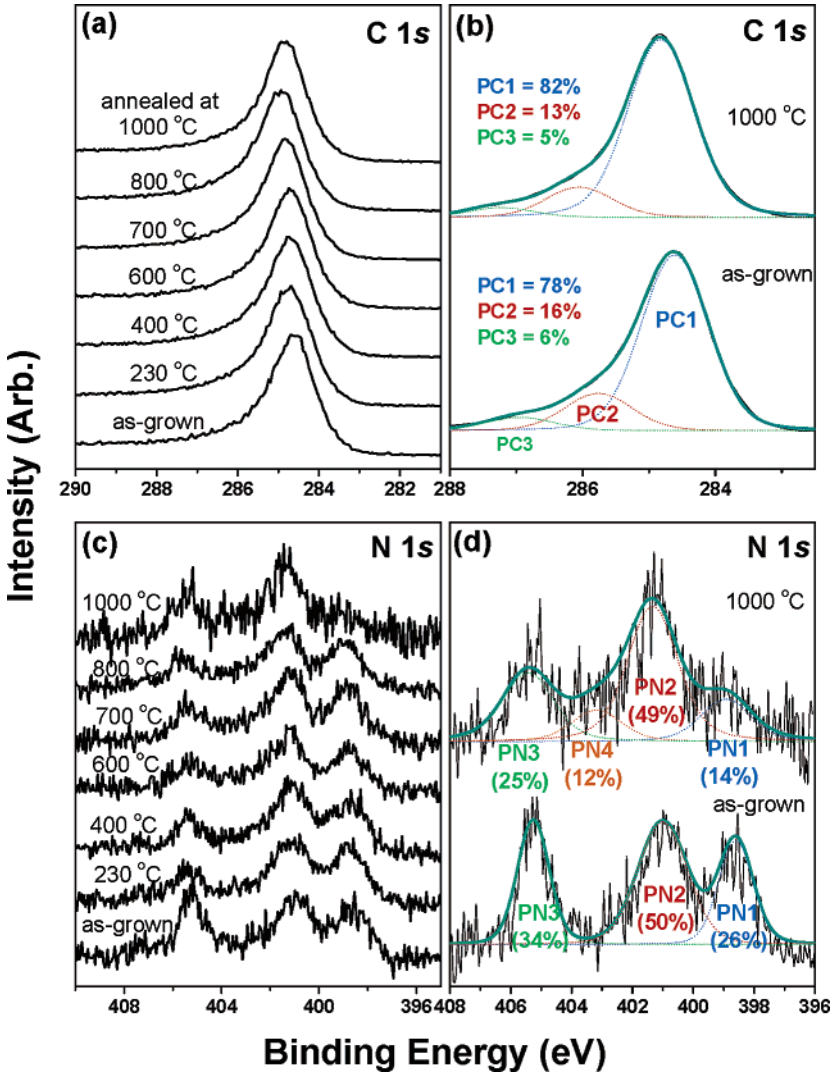

Figure 3. (a) C 1s XPS spectrum of the N-doped CNTs annealed at various temperatures up to 1000 °C. (b) Curve fitting of the C 1s band for as-grown and annealed CNTs at 1000 °C; the data (black solid line) have been curve-fitted (cyan solid line) by three Voigt profiles (PC1, PC2, and PC3, as denoted by the dotted lines). (c) N 1*s* XPS spectrum of the N-doped CNTs annealed at various temperatures up to 1000 °C. (d) Curve fitting of the N 1s normalized band for as-grown and annealed CNTs at 1000 °C; the data points (black solid line) have been curve-fitted (cyan solid line) by three Voigt profiles (PN1, PN2, and PN3) for the 1000 °C data or four Voight profiles (PN1, PN2, PN3, and PN4) for the as-grown data (Voight profiles denotes by dotted lines).

the N atoms as well as the oxygen contaminants are depleted via the annealing process.

The N 1s spectrum changes more sensitively with the annealing than the C 1s spectrum, as shown in Figure 3c. The splitting of the N 1s peak at ~400 eV indicates that the doped N atoms are in at least three different electronic structures. For the as-grown CNTs, the N 1s peak can be deconvoluted into three bands: PN1, PN2, and PN3, at 398.4, 400.2, and 405.2 eV, respectively (see Figure 3d). The respective area composition is 26%, 50%, and 34%. According to the previous XPS works of N-doped CNTs,[6,7,10] the PN1 and PN2 components can be assigned to the N atoms of pyridine-like and graphite-like structures, respectively. The higher-binding energy PC3 band is presumably ascribed to molecular N_2, which was confirmed by the following XANES data.[20,21] Considering the wall thickness (~10 nm) and inelastic mean free path (~2.5 nm) of N 1s photoelectrons at 1265 eV, the detection of PN3 suggests that molecular N_2 could be intercalated between the graphite layers at the walls.

Below 800 °C, the spectral feature of the annealed CNTs is similar to that of the as-grown CNTs, except for a reduced intensity of PN3 (see Figure 3c). This implies that the molecular N_2 that is weakly bonded to the graphite layers is first released during the annealing process; however, there is no noticeable variation in the electronic structure of the chemically bonded N atoms (PN1 and PN2). After heating at 1000 °C, the relative intensity of PN2/PN1 increases significantly, because of the removal of the pyridine-like N structures. For the quantitative comparisons, we performed a curve fitting of the N 1s spectrum, using four bands: PN1 (pyridine-like), PN2 (graphite-like), PN3 (intercalated N_2), and PN4, as shown in Figure 3d. The area composition of PN1, PN2, PN3, and PN4 is 14%, 49%, 25%, and 12%, respectively. Although the atomic percentage of PN4 is negligibly small, it can be tentatively assigned to some N-oxidic species.[22,23] They were possibly formed by the reaction of N atoms with oxygen contaminants or oxide substrates at the elevated temperatures. After annealing at 1000 °C, the area percentage of PN1 decreases, whereas that of PN2 remains the same. This result is consistent with the band assignment that the pyridine-like structures have a lower binding energy than the graphite-like structures. Shimoyama et al. examined the thermal stability of carbon nitride (CN_x) film with annealing.[24]

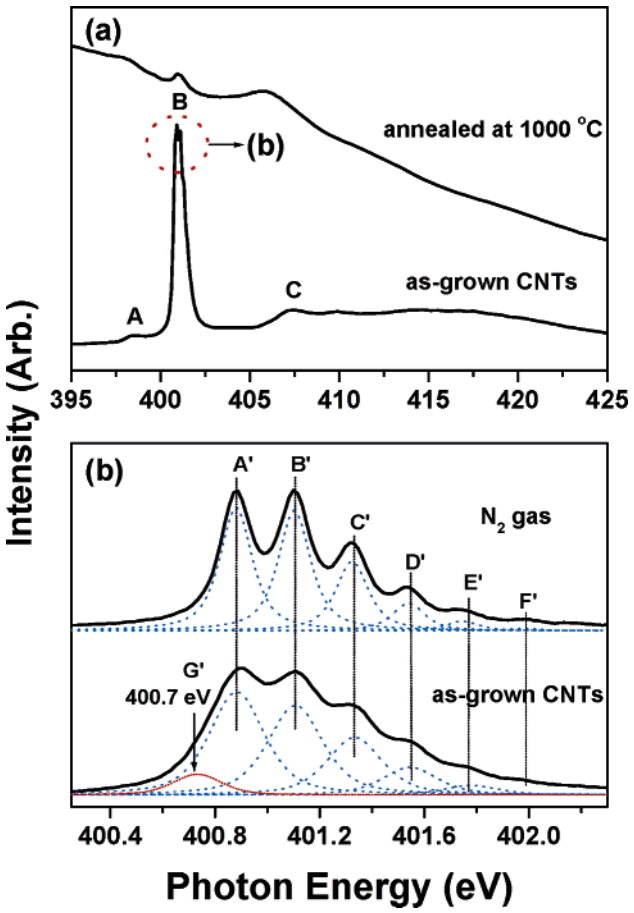

Figure 4. (a) N K-edge XANES spectrum of the as-grown and annealed CNTs at 1000 °C. (b) High-resolution XANES spectrum of the B feature. The XANES spectrum (solid line) is deconvoluted into seven peaks, labeled as A′−G′ (dotted lines), by the fitting of Voigt profiles.

They observed that the pyridine-like structures decrease and the graphitelike structures become dominant by the annealing at 1100 °C. For the CNTs, the graphitelike structures are also more stable than the pyridine-like structures.

For the annealed CNTs at 1000 °C, the peak position of PN1, PN2, and PN3 shift slightly toward higher binding energies and their bandwidths become broader, compared to those of the as-grown CNTs. The shift and broadening of N 1s peak are often observed in the CN_x film during the annealing process, which was correlated with the more-diverse local bonding environments.[25,26] It is expected that the depletion of N atoms induces the variation of local bonding environments, resulting in the electronic perturbation of core electrons. The formation of the terminating N-oxidic species may also affect the bonding environments.

The N K-edge XANES measurement was performed on the as-grown and annealed CNTs, to confirm the electronic structures of doped N atoms. It is noted that XANES can give more averaged information on the electronic structures of CNTs, because of the longer probing depth than that of XPS, which is ~10 nm.[27,28] Figure 4a shows the N K-edge XANES spectrum of the as-grown and annealed CNTs at 1000 °C. It consists of three features, centered at 398.4, 401, and 407.3 eV, labeled as A, B, and C, respectively. It is well-known that the transitions from 1s into unoccupied π^* orbitals of pyridine-like and graphitelike N structures of CN_x film usually appear at 398.3 and 400.7 eV, respectively.[24,29] The π^* feature of N_2 gas is identified at 401.1 eV. Furthermore, a careful examination reveals that the B feature splits into a fine structure that is usually observed in the vibrational fine structure of the π^* resonance of N_2 gas.[30,31] Therefore, the A feature is assigned to the π^* features of pyridine-like structures, and the B feature is an overlap of the π^* features of graphitelike structures and molecular N_2. The broad C feature can be assigned to the transitions from 1s into unoccupied σ^* orbitals.

Figure 4b shows the high-resolution spectrum of the B feature in the range of 400.2−402.3 eV. The XANES spectrum of N_2 gas is shown for comparison. The spectrum of CNTs is deconvoluted into seven peaks (labeled as A′−G′), assuming Voigt profiles. The position of resolved peaks clearly shows that the A′−F′ peaks of molecular N_2 and the peak G′ at 400.7 eV correspond to the graphitelike structures. From the relative intensity of resolved peaks, we can deduce that the molecular N_2 contributes mainly to the B feature. To the best of our knowledge, the vibrationally resolved XANES spectrum of molecular N_2 in the CNTs has not been reported until now. The widths of the resolved peaks are broader than those of pure N_2 gas. This broadening can be explained by the electronic interaction between the molecular N_2 and the CNT matrix.[32] Taking into account the probing depth of XANES, which is comparable to the average wall thickness, the most intense B feature implies that the N atoms exists mainly as molecular N_2 intercalated at the walls and trapped inside the compartments of the bamboolike structure. For the CNTs that have been annealed at 1000 °C, the B feature decreases dramatically in intensity, with no vibrational features. This observation indicates that the molecular N_2 could be released, following the tube opening.

Figure 5a displays the EELS (or energy-filtered TEM) imaging of as-grown nanotubes whose diameter is 40 nm. The N elemental mapping uses the energy loss of the K-shell edges of N (ΔE = 400 eV). The brighter points represent a higher concentration of the element, showing that the N components exist concentrated at the inner walls and the compartment region. The N elemental mapping of nanotube annealed at 1000 °C is shown in Figure 5b. The N concentration decreases particularly in the compartment region. Figure 5c shows the corresponding EELS spectrum for the as-grown and annealed nanotubes. It shows two distinct absorption features, corresponding to C−K and N−K. A detailed inspection of the near-edge fine structure confirms the sp^2 hybridization state for C, which is distinguished by a sharply defined π^* at 288 eV and a broad σ^* feature. The inset magnifies the remarkably different N−K edge features of as-grown CNT from that of annealed one; a strong peak of N_2 at 401 eV overlaps on the π^* peak (399 eV) of N atoms incorporated into sp^2-graphite frameworks. The annealed CNTs show only N sp^2 π^* and σ^* (408 eV) peaks. These data undoubtedly indicate that molecular N_2 exists inside the as-grown nanotubes, dominantly as the intercalated and trapped forms. The N atomic content is determined to be >20 at. %, which is similar to the highest N content reported so far.[33]

We measured the Raman spectroscopy of the as-grown and annealed CNTs at 1000 °C, to obtain the information about the averaged crystallinity of entire CNTs. The spectrum consists of two bands, at ~1590 cm^{-1} (G band) and ~1350 cm^{-1} (D band), that are originated from the Raman active in-plane atomic displacement E_{2g} mode and disorder-induced features, because of the finite particle size effect or lattice distortion, respectively.[34] Thus, the intensity ratio of the D band to the G band (I_D/I_G) has a linear relation with the inverse of the in-plane crystallite dimension. The value of I_D/I_G is ~0.75 for both as-

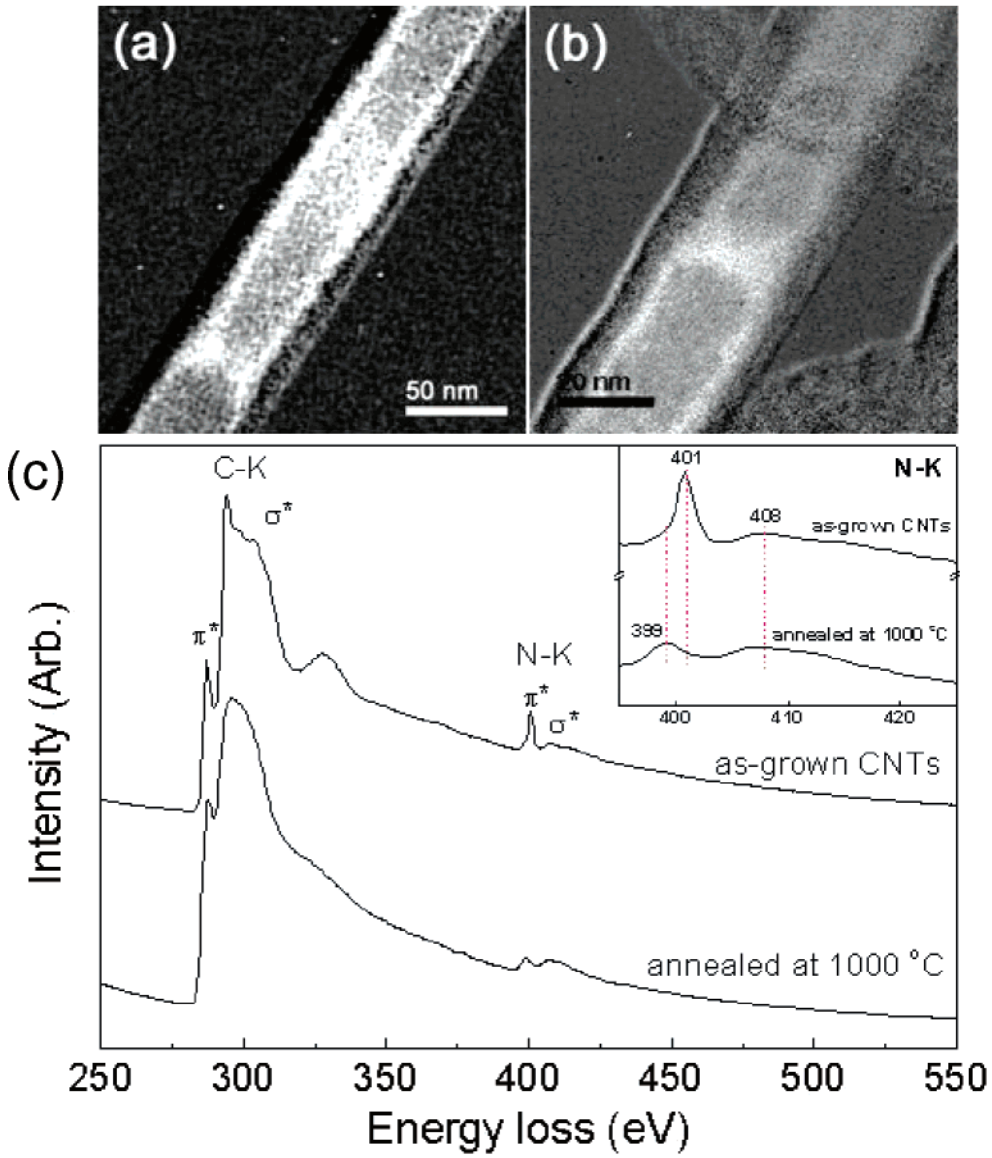

Figure 5. Elemental map of N atoms for (a) as-grown and (b) annealed CNTs at 1000 °C, obtained by EELS imaging using inelastic electrons, corresponding to the energy loss of the N−K edge. (c) EELS spectrum showing the features of C−K and N−K; the inset magnifies the N−K edge, showing the N_2 peak at 401 eV for as-grown CNT.

grown and annealed CNTs. The annealing releases mainly molecular N_2, so the value of I_D/I_G may not change much.

All of our data strongly support the abundance of N atoms inside the hollow core of CNTs, which was reported previously by several research groups.[8,35−39] The presence of N_2 is very consistent with the EELS data of the Terrones group.[8,39] Moreover we suggest that N_2 would exist dominantly as the intercalated/trapped forms, based on the XPS, XANES, and EELS data. To explain how molecular N_2 can be intercalated/trapped in the CNTs, let us conjecture the growth mechanism of the present CNTs. The closed tip without the capped catalytic particles indicates that the CNTs would be grown out from the catalytic particles deposited on the substrates. Thus, the growth would follow a typical base-growth mechanism, as suggested by other research groups.[40,41] Using the temperature-dependent growth rate data, our group proposed that the dissolved N atoms in the catalytic Fe nanoparticles would produce the N doping of the graphite sheets.[15,38] The bulk diffusion rate and the dissolved concentration of N atoms determine the N content and influence the structure of CNTs. According to the available phase diagram, the saturated N concentration reaches to 8 at. % in γ-Fe at 900 °C.[42] The precipitation and encapsulation of molecular N_2 can proceed via the following scenario. The C/N atoms dissolve into the liquid Fe nanoparticles and diffuse through them. As the C/N atoms saturate into the nanoparticles, they both precipitate and form the N-doped graphitic sheets of the wall and compartment layers. The molecular N_2 can be generated during the precipitation and intercalated/trapped in the inside of the compartments as well as the inner walls. Terrones group also proposed a similar encapsulation process of N_2 in the compartments using a base-growth model, for the CNTs produced via the pyrolysis of ferrocene and benzylamine.[39]

IV. Conclusions

We have investigated the electronic structures of N atoms that have been doped in the carbon nanotubes (CNTs) and the annealing effects on their electronic structures using Xray photospectroscopy (XPS), X-ray absorption near-edge spectroscopy (XANES), and electron energy loss (EELS) techniques. The bamboolike structured CNTs were synthesized by the pyrolysis of iron phthalocyanine ($FeC_{32}N_8H_{16}$, FePc) at 900 °C.

The average diameter and wall thickness were 50 and 10 nm, respectively. The XPS analysis revealed that the average N content decreased from 6.3 at. % to 3.3 at. % via the annealing at 1000 °C. For the as-grown CNTs, the N 1s XPS spectrum showed that the N atoms were in at least three different electronic structures; graphitelike, pyridine-like, and molecular N_2. The vibrationally resolved π^* feature of the XANES spectrum decisively indicated the existence of molecular N_2, which could be intercalated at the walls and also trapped in the compartments. The EELS analysis confirmed the release of molecular N_2, which was due to the annealing. During the annealing process at <800 °C, the electronic structures of chemically bonded N atoms remained almost the same, although the N content significantly decreased, mainly because of the release of molecular N_2. With annealing at 1000 °C, the pyridine-like structures deplete notably, reflecting a lower thermal stability, compared to the graphitelike structures. A base-growth model was suggested to explain how molecular N_2 can be intercalated and trapped. Detailed understanding of the electronic structures and thermal stability of N-doped CNTs will lead to the tailoring of CNTs to suit the applications of field-emission sources and nanoelectronic devices.

Acknowledgment. This work was supported by the Korea Science and Engineering Foundation (Project No. R14-2004-033-01003-0; R02-2004-000-10025-0) and the Korea Research Foundation (Project No. 2004-015-C00265). H.-J. Shin and H. J. Song acknowledge the partial support from Korean Ministry of Science and Technology (Project No. M1-2012-02-0003).

References and Notes

(1) Iijima, S. *Nature* **1991**, *354*, 56.
(2) Odom, T. W.; Huang, J.-L.; Kim, P.; Lieber, C. M. *Nature* **1998**, *391*, 62.
(3) Rueckes, T.; Kim, K.; Joselevich, E.; Tseng, G. Y.; Cheung, C.-L.; Lieber, C. M. *Science* **2000**, *289*, 94.
(4) Bachtold, A.; Hadley, P.; Nakanishi, T.; Dekker, C. *Science* **2001**, *294*, 1317.
(5) Saito, Y.; Hamaguchi, K.; Hata, K.; Uchida, K.; Tasaka, Y.; Ikazaki, F.; Yumura, M.; Kasuya, A.; Nishina, Y. *Nature* **1997**, *389*, 554.
(6) Sen, R.; Satishkumar, B. C.; Govindaraj, A.; Harikumar, K. R.; Renganathan, M. K.; Rao, C. N. R. *J. Mater. Chem.* **1997**, *7*, 2335.
(7) Terrones, M.; Redlich, P.; Grobert, N.; Trasobares, S.; Hsu, W. K.; Terrones, H.; Zhu, Y. Q.; Hare, J. P.; Reeves, C. L.; Cheetham, A. K.; Rühle, M.; Kroto, H. W.; Walton, D. R. M. *Adv. Mater.* **1999**, *11*, 655.
(8) Terrones, M.; Kamalakaran, R.; Seeger, T.; Rühle, M. *Chem. Commun.* **2000**, 2335.
(9) Wang, X.; Liu, Y.; Zhu, D.; Zhang, L.; Ma, H.; Yao, N.; Zhang, B. *J. Phys. Chem. B* **2002**, *106*, 2186.
(10) Kudashov, A. G.; Okotrub, A. V.; Bulusheva, L. G.; Asanov, I. P.; Shubin, Yu. V.; Yudanov, N. F.; Yudanova, L. I.; Danilovich, V. S.; Abrosimov, O. G. *J. Phys. Chem. B* **2004**, *108*, 9048.
(11) Jang, J. W.; Lee, C. E.; Lyu, S. C.; Lee, T. J.; Lee, C. J. *Appl. Phys. Lett.* **2004**, *84*, 2877.
(12) Ebbesen, T. W.; Ajayan, P. M.; Hiura, H.; Tanigaki, K. *Nature* **1994**, *367*, 519.
(13) Huang, W.; Wang, Y.; Luo, G.; Wei, F. *Carbon* **2003**, *41*, 2585.
(14) Koningsber, D. C., Prins, R., Eds. *X-ray Absorption*: Wiley: New York, 1988.
(15) Kim, N. S.; Lee, Y. T.; Park, J.; Han, J. B.; Choi, Y. S.; Choi, S. Y.; Choo, J.; Lee, G. H. *J. Phys. Chem. B* **2003**, *107*, 9249.
(16) Seah, M. P.; Dench, W. A. *Surf. Interface Anal.* **1979**, *1*, 2.
(17) Shirley, D. A. *Phys. Rev. B* **1972**, *5*, 4709.
(18) Moulder, J. F.; Sticks, W. F.; Sobol, P. E.; Bomben, K. D. *Handbook of X-ray Photoelectron Spectroscopy*; Physical Electronics, Inc.: Eden Prairie, MN, 1995.
(19) Beshkov, G.; Dimitrov, D. B.; Georgiev, St.; Juan-Cheng, D.; Petrov, P.; Velchev, N.; Krastev, V. *Diamond Relat. Mater.* **1999**, *8*, 591.
(20) Grunze, M. J.; Fuhler, J.; Neumann, M.; Brundle, C. R.; Auerbach, D. J.; Behm, J. *Surf. Sci.* **1984**, *139*, 109.
(21) Björneholm, O.; Nilsson, A.; Sandell, A.; Hernnäs, B.; Mårtensson, N. *Phys. Rev. Lett.* **1992**, *68*, 1892.
(22) Belz, T.; Bauer, A.; Find, J.; Günter, M.; Herein, D.; Mökel, H.; Pfänder, N.; Sauer, H.; Schulz, G.; Schütze, J.; Timpe, O.; Wild, U.; Schlögl, R. *Carbon* **1998**, *36*, 731.
(23) Ohta, R.; Lee, K. H.; Saito, N.; Inoue, Y.; Sugimura, H.; Takai, O. *Thin Solid Films* **2003**, *434*, 296.
(24) Shimoyama, I.; Wu, G.; Sekiguchi, T.; Baba, Y. *J. Electron Spectrosc. Relat. Phenom.* **2001**, *114*−*116*, 841.
(25) Chowdhury, A. K. M. S.; Cameron, D. C.; Hashmi, M. S. J. *Surf. Coat. Technol.* **1999**, *112*, 133.
(26) Zhou, Z.; Xia, L.; Sun, M. *Appl. Surf. Sci.* **2003**, *210*, 293.
(27) Schroeder, S. L. M.; Moggridge, G. D.; Ormerod, R. M.; Rayment, T.; Lambert, R. M. *Surf. Sci.* **1995**, *324*, L371.
(28) Choi, H. C.; Lee, M. K.; Shin, H. J.; Kim, S. B. *J. Electron Spectrosc. Relat. Phenom.* **2003**, *130*, 85.
(29) Shimoyama, I.; Wu, G.; Sekiguchi, T.; Baba, Y. *Phys. Rev. B* **2000** *62*, R6053.
(30) Lee, M. K.; Shin, H.-J. *Nucl. Instrum. Methods Phys. Rev. A* **2001**, *467*−*468*, 508.
(31) Ceballos, G.; Haack, N.; Wende, H.; Puttner, R.; Arvanitis, D.; Baberschke, K. *Nucl. Instrum. Methods Phys. Rev. A* **2001**, *467*−*468*, 1560.
(32) Esaka, F.; Shimada, H.; Imamura, M.; Matsubayashi, N.; Kikuchi, T.; Furuya, K. *J. Electron Spectrosc. Relat. Phenom.* **1999**, *88*−*91*, 817.
(33) Glerup, M.; Castignolles, M.; Holzinger, M.; Hug, G.; Loiseau, A.; Bernier, P. *Chem. Commun.* **2003**, 2542.
(34) Tuinstra, F.; Koenig, J. L. *J. Chem. Phys.* **1970**, *53*, 1126.
(35) Han, W. Q.; Redlich, P.; Seeger, T.; Ernst, F.; Rühle, M.; Grobert, N.; Hsu, W. K.; Chang, B. H.; Zhu, Y. Q.; Kroto, H. W.; Walton, D. R. M.; Terrones, M.; Terrones, H. *Appl. Phys. Lett.* **2000**, *77*, 1807.
(36) Suenaga, K.; Yudasaka, M.; Colliex, C.; Iijima, S. *Chem. Phys. Lett.* **2000**, *316*, 365.
(37) Trasobares, S.; Stéphan, O.; Colliex, C.; Hsu, W. K.; Kroto, H. W.; Walton, D. R. M. *J. Chem. Phys.* **2002**, *116*, 8966.
(38) Lee, Y. T.; Kim, N. S.; Bae, S. Y.; Park, J.; Yu, S.-C.; Ryu, H.; Lee, H. J. *J. Phys. Chem. B* **2003**, *107*, 12958.
(39) Reyes-Reyes, M.; Grobert, N.; Kamalakaran, R.; Seeger, T.; Golberg, D.; Rühle, M.; Bando, Y.; Terrones, H.; Terrones, M. *Chem. Phys. Lett.* **2004**, *396*, 167.
(40) Katayama, T.; Araki, H.; Yoshino, K. *J. Appl. Phys.* **2002**, *91*, 6675.
(41) Wang, X.; Hu, W.; Liu, Y.; Long, C.; Xu, Y.; Zhou, S.; Zhu, D.; Dai, L. *Carbon* **2001**, *39*, 1533.
(42) Massalski, T. B. *Binary Alloy Phase Diagrams*; American Society for Metals: Metals Park, OH, 1986.